The RSC complex remodels nucleosomes in transcribed coding sequences and promotes transcription in *Saccharomyces cerevisiae*

Emily Biernat[1], Jeena Kinney[1], Kyle Dunlap[1], Christian Rizza[1], and Chhabi K. Govind[1*]

Corresponding Author:

* Chhabi K. Govind

Mathematics and Science Building, Room 333

Department of Biological Sciences

Oakland University

Rochester

Michigan 48309

USA

[1] Department of Biological Sciences

Oakland University

Rochester

Michigan 48309

USA

SUMMARY

RSC (Remodels the Structure of Chromatin) is a conserved ATP-dependent chromatin remodeling complex that regulates many biological processes, including transcription by RNA polymerase II (Pol II). We report that not only RSC binds to nucleosomes in coding sequences (CDSs) but also remodels them to promote transcription. RSC MNase ChIP-seq data revealed that RSC-protected fragments were very heterogenous (~80 bp to 180 bp) compared to the sharper profile displayed by the MNase inputs (140 bp to 160 bp), supporting the idea that RSC activity promotes accessibility of nucleosomal DNA. Importantly, RSC binding to +1 nucleosomes and CDSs, but not with -1 nucleosomes, strongly correlated with Pol II occupancies suggesting that the RSC enrichment in CDSs is important for efficient transcription. This is further supported by a similar heterogenous distribution of Pol II-protected fragments. As such, the genes harboring high-levels of RSC in their CDSs were the most strongly affected by ablating RSC function. Altogether, this study provides a mechanism by which RSC-mediated remodeling aids in RNA Pol II traversal though coding sequence nucleosomes in vivo.

The nucleosome is the fundamental unit of chromatin and is formed by wrapping ~147 base pairs of DNA around an octamer of histones (2 copies of H3, H4, H2A and H2B). DNA wrapped around a histone octamer is inaccessible for DNA-dependent processes, including transcription by RNA polymerase II (Pol II) (Lorch et al., 1987). This nucleosomal impediment can be relieved by chromatin remodeling complexes that use the energy derived from ATP hydrolysis to slide or evict histones in order to expose the underlying DNA (Clapier and Cairns, 2009; Clapier et al., 2016). One such remodeler is the SWI/SNF family member RSC (remodels the structure of chromatin) complex, the only essential remodeler in budding yeast (Cairns et al., 1996).

RSC is an important regulator of chromatin organization around gene promoters. It is implicated in establishing 'nucleosome depleted regions' (NDRs) found upstream of transcription start sites (TSSs) and also in positioning of the NDR-flanking nucleosomes referred to as the -1 and +1 nucleosomes (Nuc) (Krietenstein et al., 2016). The DNA sequence forming the +1_Nuc often harbors TSS, and +1_Nuc can therefore be inhibitory for transcription initiation. RSC has been shown to bind both the -1_Nuc and +1_Nuc, and impairing RSC function is associated with the movement of flanking nucleosomes toward the NDR, which results in filling of the NDRs (Badis et al., 2008; Brahma and Henikoff, 2019; Ganguli et al., 2014; Hartley and Madhani, 2009a; Klein-Brill et al., 2019; Kubik et al., 2015; Rawal et al., 2018). Nucleosomes which invade or assemble within NDRs are also cleared by RSC (Brahma and Henikoff, 2019; Kubik et al., 2015). These nucleosomes were bound by RSC and were termed "fragile", given their greater sensitivity to digestion by micrococcal nuclease (MNase). The presence of such nucleosomes is controversial, partly due to the difficulty in detecting them by conventional ChIP-seq methods (Chereji et al., 2017). Moreover, the importance of fragile nucleosomes in transcription is not clear. In addition

to RSC, general regulatory factors (GRFs) and underlying DNA sequences play a role in NDR formation and maintenance (Krietenstein et al., 2016; Kubik et al., 2018).

The role of RSC in regulating chromatin structure at promoters is also linked to its role in transcription. When cells were depleted of the catalytic RSC subunit Sth1, the resulting shift in nucleosomes towards NDRs was associated with reduced Pol II and TBP occupancies at a subset of genes (Kubik et al., 2018; Rawal et al., 2018), and reduced TSS utilization and transcription (Klein-Brill et al., 2019; Kubik et al., 2019). RSC is also suggested to play a post-initiation role in promoting transcription. For example, RSC promoted Pol II elongation through acetylated nucleosomes *in vitro* (Carey et al., 2006), and RSC localizes to transcribed coding sequences (CDSs) in vivo (Ganguli et al., 2014; Spain et al., 2014). Cells deficient for both RSC (Sth1) and SWI/SNF (Snf2) displayed reduced Pol II occupancy at targets of Gcn4 under conditions of amino acid starvation (Rawal et al., 2018). Notably, the CDSs of Gcn4 targets were also enriched for RSC (Spain et al., 2014) and SWI/SNF (Rawal et al., 2018). Moreover, depleting Rsc8 (RSC subunit) altered distribution of Pol II along coding regions (Ocampo et al., 2019). These results suggest that the role of RSC in promoting transcription might extend to post-initiation steps, and could include remodeling nucleosomes immediately downstream of elongating Pol II in CDSs.

To address a potential role for RSC in promoting transcription by increasing DNA accessibility in CDSs, we performed ChIP-seq using MNase-digested chromatin and mapped RSC at nucleosomal resolution. We then analyzed the length of DNA associated with RSC-bound nucleosomes (RSC_Nucs). We found that RSC was enriched in many promoters and also in CDSs of highly transcribed genes. RSC_Nucs were very sensitive to MNase digestion, displaying a more heterogenous size distribution (~80 – 180 bp) compared to canonical nucleosomes, which showed

a relatively sharp profile (~140 - 160 bp). This suggests not only that does RSC bind to nucleosomes in CDSs but also remodels them to makes them susceptible to MNase digestion. Such nucleosomes might therefore be more accessible to transcribing polymerases. In support of this idea, we found that Pol II-bound nucleosomes (Pol II_Nucs) were very sensitive to MNase-digestion. Furthermore, the genes that showed RSC enrichment in their coding sequences, but not their promoters, showed the greatest reductions in transcription on RSC depletion. Overall, our data support a model in which RSC makes gene-body nucleosomes accessible, thus lowering the barrier to Pol II traversal and promoting efficient transcription.

RESULTS

Nucleosomes in transcribed coding sequences are sensitive to MNase digestion

DNA is relatively more resistant to MNase digestion when it is wrapped around the histone octamer or protected by non-histone proteins. As such, sequencing of the MNase-protected DNA fragment (MPDFs) is widely used to determine precise nucleosome occupancy and positioning (Koerber et al., 2009; Ramachandran et al., 2017). Considering that nucleosomes inhibit transcription by limiting access to DNA, we sought to determine the location of accessible nucleosomes, and whether the presence of such nucleosomes correlates with transcription. To this end, we digested formaldehyde cross-linked chromatin with MNase and subjected the purified DNA to paired-end deep sequencing (Figure S1A and S1B).

The majority of DNA fragment lengths from the MNase-digested chromatin was between 100 and 200 bp, with the peak centered around 150 bp (Figure 1A), consistent with amount of DNA protected by canonical nucleosomes (Henikoff et al., 2011; Ramachandran et al., 2017;

Ramachandran and Henikoff, 2016a). A heatmap showing normalized MNase-seq read density for all fragments for yeast genes (5764 genes) displayed NDRs upstream of the TSS (Figure 1B and Figures S1A and S1B). The genes were sorted in descending order by the average Pol II occupancy in their CDSs determined by Rpb3 ChIP-seq from sonicated chromatin (Figure 1C and Figure S1C). As expected, the highly transcribed genes exhibited lower nucleosome occupancies in their promoters and CDSs, and also displayed wider NDRs (Figure 1B and 1C; compare the top of the heatmaps). These results are consistent with the idea that histones are evicted both from promoters and from CDSs in the course of transcription, especially in highly-transcribed genes (Dion et al., 2007).

Unwrapping of nucleosomal DNA by remodelers or the ejection of H2A/H2B dimers could make the nucleosomal DNA more susceptible to digestion by MNase yielding MPDFs shorter than 147 bp as shown previously (Brahma and Henikoff, 2019; Ramachandran et al., 2017) (Figure 1D). To determine the abundance of shorter fragments genome-wide, we analyzed MNase-seq data according to different MPDF lengths. A smaller enrichment for the shorter MPDFs over the canonical nucleosomes was evident for almost all nucleosomes (Figure 1E, compare black trace with other colored traces). However, the most enrichment for the shorter MPDFs (<120 bp) was evident at the -1 and -2 positions, similar to what was observed in *Drosophila* cells (Ramachandran and Henikoff, 2016b; Ramachandran et al., 2015). Shorter MPDFs at the -1 and -2 positions might reflect the chromatin remodeling that ensues during transcription in the promoter-proximal regions upstream of NDRs. Enrichment of H2AZ in nucleosomes at -1 and +1 positions could also results in shorter MPDFs considering that H2AZ makes nucleosomes less stable (Weber et al., 2014). For

simplicity, we will refer to particles generating shorter MPDFs (<120 bp) as sub-nucleosomal particles.

We next asked whether the CDSs of highly-transcribed genes display greater abundance of shorter MPDFs. To this end, we analyzed genes with the top 10% (Pol II-T10) and the bottom 10% (Pol II-B10) of Pol II occupancies for MPDFs >130 bp and <120 bp (Figure 1F). We found that the Pol II-B10 genes displayed higher canonical nucleosome occupancies compared to Pol II-T10 genes (Figure 1F; compare dark red and dark blue traces), and also displayed enrichment of MPDFs >130 bp over <120 bp (compare dark and light red traces) at the +2 to +6 positions. In contrast, the Pol II-T10 genes showed a higher enrichment of the shorter fragments (<120 bp vs >130 bp; light and dark blue traces) both in CDSs as well as in promoters. These results suggest that the nucleosomes in the transcribed CDSs (Pol II-T10) are more accessible to MNase compared to those in non-transcribed CDSs (Pol II-B10). These results are consistent with the idea that nucleosomes in transcribed CDSs are either actively remodeled or converted to hexasomes, which have been shown to allow Pol II traversal through chromatin templates *in vitro* (Kireeva et al., 2002; Kulaeva et al., 2007) and are shown to be present in vivo (Ramachandran et al., 2017).

RSC Localizes to nucleosomes of highly transcribed genes

RSC plays important roles in maintaining NDRs near promoter regions (Krietenstein et al., 2016; Kubik et al., 2015; Kubik et al., 2017; Musladin et al., 2014), and has been implicated in promoting transcription (Carey et al., 2006; Ganguli et al., 2014; Ocampo et al., 2019; Rawal et al., 2018; Spain et al., 2014; Spain and Govind, 2011). The ability to slide nucleosome to widen NDRs appears to enhance PIC assembly and the TSS selection (Klein-Brill et al., 2019; Kubik et al.,

2019). In addition, it may promote transcription by facilitating transcription elongation (Carey et al., 2006; Spain and Govind, 2011). In support of this possibility, we had previously provided genome-wide (ChIP-chip) evidence for localization of RSC in transcribed CDSs (Spain et al., 2014; Spain and Govind, 2011), which has subsequently been observed by other groups (Ganguli et al., 2014; Vinayachandran et al., 2018). Considering that RSC is enriched in CDSs of many transcribed genes, we sought to determine whether RSC remodels nucleosomes in CDSs. To this end, we ChIP-ed a myc-tagged form of Sth1, the catalytic subunit of the RSC complex, from MNase-digested chromatin and performed deep sequencing. In agreement with earlier studies (Spain and Govind, 2011; Yen et al., 2012), we observed a robust enrichment of RSC in the CDSs of many genes showing high Pol II occupancies including ribosomal protein genes (RPGs) (Figures 2A and S2A). The highest RSC occupancy in CDSs was for the genes displaying greatest Pol II occupancies (Figures 2B and S2A). Additionally, the Pol II-T10 genes displayed a substantial overlap to those with the top 10% RSC occupancy in CDSs (RSC-T10 genes henceforth; p-value = 4.8×10^{-333}) (Figure S2B and S2C). These results indicate that the majority of highly transcribed genes are enriched for RSC in their CDSs.

RSC occupancy normalized to nucleosomes clearly revealed that the Pol II-T10 genes are highly enriched for RSC in their CDSs with relatively low occupancies in promoters (Figure 2C, top-middle panel and Figure 2D, top panel). Since several studies, including ours, have shown that RSC is enriched at promoters of many genes (Badis et al., 2008; Brahma and Henikoff, 2019; Kubik et al., 2018; Spain et al., 2014; Yen et al., 2012). To identify those genes whose promoters are enriched for RSC, we calculated RSC occupancies in the regions encompassing NDRs and -1_Nuc, and selected the top 10% of such genes (henceforth “Pro-targets”; Figure 2C, top-right

panel). Pro-targets displayed higher RSC occupancies in promoters versus CDSs. It is worth noting that RSC occupancies were substantially higher in Pol II-T10 and Pro-targets than those observed in the Pol II-B10 genes.

We also noted that the RSC-T10 and Pol II-T10 genes showed very similar RSC profiles in the CDSs, raising a strong possibility that presence of RSC in CDSs is linked to transcription (Figure 2D; top panel, compare yellow and red traces). As such, Pol II occupancies, genome-wide, strongly correlated with RSC occupancies in CDSs (ρ =0.86; R^2 = 0.71) and only weakly in promoters (ρ =0.26; R^2 = 0.01) (Figure 2E). Many recent studies have shown that RSC is important for maintaining NDRs genome-wide (Brahma and Henikoff, 2019; Ganguli et al., 2014; Hartley and Madhani, 2009b; Kubik et al., 2015; Kubik et al., 2017; Kubik et al., 2018). However, low correlation between RSC occupancies in promoters would suggest that keeping NDRs free of nucleosomes might be a general function of RSC and not necessarily linked to high-level of transcription.

The Pro-targets exhibited lower nucleosome occupancies in their promoters compared to the Pol II-B10 promoters (Figure 2C; bottom-right vs bottom-left panels). Lower nucleosome occupancy at Pro-targets is consistent with the role of RSC in evicting nucleosomes from promoters on its own and in cooperation with the SWI/SNF complex (Rawal et al., 2018). Intriguingly, however, the Pro-targets' NDR depth was nearly identical to that of the Pol II-T10 genes. The Pol II-T10 genes are expected to have the broadest NDRs considering that high-level transcription is often associated with histone eviction from the promoters. However, Pro-targets displayed substantially lower Pol II occupancies in their CDSs (Figure 2F and Figure S2D). Therefore, it appears that

deeper NDR depth for the Pro-targets is unlikely driven by transcription activity. Another possibility could be that the Pro-targets promoter regions might be dAdT-rich. It has been shown that dAdT-rich sequences exclude nucleosomes and are more sensitive to MNase digestion (Chereji et al., 2018; Suter et al., 2000). However, the dAdT content +/- 250 bp around TSS of the Pro-targets, Pol II-T10 and Pol II-B10 genes was not significantly different (Figure S2E). We therefore favor the idea that RSC occupancy at Pro-targets might remove nucleosomes from NDRs of Pro-targets. Consistent with this idea, both the +1_Nuc and -1_Nuc are shown to be enriched for RSC genome-wide (Brahma and Henikoff, 2019; Krietenstein et al., 2016; Kubik et al., 2017).

To get the better idea about the relationship between transcription and the presence of RSC in promoters and in CDSs, we calculated RSC occupancies at +1_Nuc and -1_Nuc, genome-wide. Interestingly, RSC occupancy at +1_Nuc strongly correlated with Pol II occupancies (ρ =0.58; R^2 = 0.50) compared to RSC occupancy at -1_Nuc (ρ = 0.2; R^2 = 0.01) (Figure 2G). This suggests that RSC recruitment to the +1_Nuc is coupled to transcription. The data so far suggest that high RSC occupancies in promoters enhances NDR formation, but elevated RSC occupancies in CDSs are much more predictive of high-level of transcription.

RSC-bound nucleosomes are more susceptible to MNase

Considering that nucleosomes in both promoters and CDSs displayed the presence of shorter MPDFs, we asked whether RSC preferentially associates with intact nucleosomes (>130 bp) or with partially unraveled / subnucleosomes (<130 bp). While the MNase-inputs for Pol II-B10 genes displayed very similar levels of both nucleosomal and subnucleosomal particles (Figure 3A), enrichment for the nucleosomal fraction was slightly higher for the RSC-bound nucleosomes

(RSC_Nucs) (Figure 3A; compare red vs orange traces). Thus, there was a very little enrichment of fragments corresponding to subnucleosomal particles in RSC_Nucs for the Pol II-B10.

The MNase inputs for the Pol II-T10 displayed a slightly higher proportion of sub-nucleosomal particles than the nucleosomes (Figure 3B; compare black and grey traces). However, the overall levels were very similar to Pol II-B10 genes (compare Nucs in Figure 3A and 3B, and Figures S3A and S3B). By contrast, both nucleosomal and subnucleosomal particles were substantially enriched in the RSC_Nucs compared to the MNase inputs (Figure 3B; gray and black traces). However, the RSC_Nucs were relatively more enriched for shorter fragments vs nucleosome-size fragments (Figure 3B, compare orange vs red traces). We also noted that the positioning of the RSC_Nucs appeared to be more diffused suggesting that RSC_Nucs could be more dynamic compared to canonical nucleosomes.

The higher proportion of shorter MPDFs in RSC_Nucs raised the possibility that elevated RSC occupancy and attendant remodeling makes nucleosomes more susceptible to MNase. To get a better idea of the distribution of DNA fragment sizes associated with RSC_Nucs, we performed a two-dimensional (2-D) analysis of fragment-length distributions (Chereji et al., 2017) of RSC_Nucs at the Pol II-B10, Pro-targets, and Pol II-T10 genes, which showed high-level RSC occupancy in their CDSs and compared them to the fragment-length distributions for all nucleosomes (MNase inputs) at the same gene-sets. Such comparison allowed us to differentiate the remodeling status of RSC_Nucs from other nucleosomes in same region. Both the promoters and CDSs of the Pol II-T10 genes, and the promoters of the Pro-targets, displayed lower nucleosome densities compared to the corresponding regions of the Pol II-B10 genes (Figure 3C). Despite the differences in the nucleosome densities (MPDFs ~150 bp), the fragment size

distributions for the total nucleosomes at these three gene-sets were similar (Figures 3C and 3E, left panel). There were no major differences between the fragment length distributions of total nucleosomes and RSC_Nucs at the Pol II-B10 genes (Figure S3C). In contrast, the Pro-targets, and the Pol II-T10 genes displayed a substantially higher proportion of shorter fragments in RSC_Nucs versus total nucleosomes (Figures 3C-D and Figures S3D-E), and in comparison, to the RSC_Nucs at the Pol II-B10 genes (Figures 3C-E, blue vs. red and black traces, and Figures S3D and S3E, compare red and blue traces). More importantly, the distribution of shorter fragments coincided with the RSC occupancies: the majority of the shorter fragments were localized in the region upstream of the TSS for the Pro-targets where RSC occupancies are highest; whereas, for the Pol II-T10 genes the shorter fragments were localized in the CDSs, where the majority of RSC is found. The abundance of shorter fragments also largely corresponded to RSC occupancies (Figure 3E). As such, the highest levels of shorter fragments were observed for the ribosomal protein genes (RPGs), followed by the Pol II-T10 genes. It is notable that the size distributions for the RSC_Nucs were very broad and relatively smooth as opposed to the discrete-sized fragments observed upon MNase over-digestion (Chereji et al., 2018). Such profiles fit with the remodeling activity of RSC, which gradually exposes DNA through its translocase activity (Clapier et al., 2016). The upper limit of MPDFs (~180 bp) in RSC_Nucs could be due to the protection provided due to formation of the RSC-nucleosome complex (Shukla et al., 2010) whereas shorter MPDFs might be representative of partially unwrapped nucleosomes or hexasomes (Brahma and Henikoff, 2019).

It is also important to note that the fragment size distributions of nucleosomes (MNase inputs) and RSC_Nucs were very different even at the most highly transcribed genes, for e.g. RPGs (Figures S3A and S3B, the two right-most panels). The overall fragment-size profiles for total nucleosomes in both non-transcribing and transcribing genes are very similar (Figure 3E, left panel), suggesting

that remodeled nucleosomes represent only a small fraction of total nucleosomes in CDSs even at the highly transcribing genes. Altogether, a greater fraction of shorter fragments associated with RSC_Nucs strongly suggest that RSC binding renders nucleosomes accessible in a manner that makes them more accessible to MNase digestion than canonical nucleosomes, and potentially enhances transcription elongation.

RNA polymerase Interacts with MNase-Sensitive Nucleosomes In Vivo:

Earlier studies have shown that Pol II tends to localize close to nucleosomes in coding regions (Churchman and Weissman, 2011), and has been shown to interact with nucleosomes by MNase ChIP-seq (Koerber et al., 2009). Considering that DNA from RSC_Nucs displayed very heterogenous fragment sizes and that RSC has been shown to enhance transcription *in vitro* through acetylated chromatin templates (Carey et al., 2006), we sought to examine the accessibility of Pol II-bound nucleosomes. To this end, we performed Rpb3 (Pol II) ChIP-seq using MNase digested chromatin and examined Rpb3 ChIP-seq signals for MPDF length between 130-160 bp to ensure that the nucleosomal-length fragments were ChIP-ed with Pol II (Figure 4A). The Pol II MNase ChIP-seq occupancy profile highly correlated with the Pol II occupancies determined by Rpb3 ChIP-seq analysis of sonicated chromatin (r=0.84) (compare Figure 4A and Figure 1C, and Figure 4B), suggesting that Pol II indeed interacts with nucleosomes and not merely naked DNA within in transcribed CDSs.

We next examined the fragment size distribution for the Rpb3-bound nucleosomes (Rpb3_Nucs henceforth). The Rpb3_Nucs MPDF size distribution profile for the Pol II-T10 genes (Figure 4C) was very similar to that observed for the RSC_Nucs (Figure 3D). The frequent association of Pol

II with subnucleosomal fragment length <130 bp suggests that MNase ChIP-seq captures the Pol II molecules that are interacting with or traversing through nucleosomes. This possibility is consistent with the recent cryo-EM structures of Pol II transcribing through nucleosomes (Farnung et al., 2018; Kujirai et al., 2018). The similarity between the size distribution of the Pol II_Nucs (Figures 3D, right panel and Figure 4C), and the strong correlation between RSC and Pol II occupancies (Figure 4E), suggest that Pol II bound to partially unwrapped nucleosomes or hexasomes might have been remodeled by RSC. If so, one might expect to see transcription defects upon ablating RSC function, especially at those genes which show high RSC occupancies in their CDSs.

Ablating RSC transcription of highly transcribed genes

To test the above prediction, we examined the Pol II ChIP-seq data from isogenic WT and Rsc8-depleted cells (*rsc8*), published by Clark and colleagues (Ocampo et al., 2019). We observed that the reductions in Pol II occupancies upon Rsc8 depletion were greatest at genes displaying the highest Pol II occupancies in WT cells, genome-wide (Figure 4D and 4E). The reductions negatively correlated with RSC occupancy in CDSs (ρ = -0.38) but not with RSC levels in promoters (ρ = 0.02) in WT cells, indicating that the most highly transcribed genes, which also tends to harbor RSC at high-levels in their CDSs, are the most affected by impairing RSC function (Figure 4D). Among the top 10% of the genes showing the greatest reduction in Pol II occupancies in their CDSs upon Rsc8 depletion (RSC-affected henceforth), approximately 67% (388 of 576; p-value = 2.6×10^{-306}) were Pol II-T10 genes (Figure 4SA). Depletion of Rsc8 elicited very similar reductions in Pol II occupancies in Pol II-T10 and RSC-T10 genes (Figure 4E). By contrast, only 75 of 576 Pro-target genes were among the RSC-affected genes (Figure S4A), and displayed only

minimal defects in Pol II occupancy, which mirrored the defects observed genome-wide (Figure 4E; Pro-targets vs all genes). The analyses thus far suggest that transcription of the genes harboring high-levels of RSC in CDSs are the most affected upon impairing RSC function (Figure S4B). Altogether, the data suggest that the role of RSC in promoting nucleosome accessibility in CDSs is important for transcription.

To understand the extent to which these defects are caused by changes in chromatin structure, we analyzed MNase-seq data from WT and *rsc8* cells (Ocampo et al., 2019). Nucleosomes in both Pol II-B10 and RSC Pro-targets genes moved towards the NDRs in *rsc8* cells, leading to shallower NDRs (Figure 4F). Both gene-sets showed filled NDRs to a very similar extent, despite the fact that Pro-targets exhibited higher Pol II occupancies in their CDSs (Figure 2F). This observation suggests that maintaining appropriate NDR width is a general function of RSC in a manner that is independent of transcription status. In contrast, *rsc8* elicited a relatively small effect on the NDR filling for the highly transcribed Pol II-T10 genes (Figure 4G), despite these genes showing the greatest reductions in Pol II occupancies in *rsc8* cells. Depletion of Rsc8 was shown to be associated with increases in Pol II occupancies towards the 3'ends of transcribed genes (Ocampo et al., 2019) (Figure S4C and S4D). Although a relatively minor shift in +1 nucleosomes in *rsc8* could lower Pol II occupancies in CDSs (Figure 4F), but it does not fully explain the altered profile of Pol II observed in rsc8 cells. It is reasonable to propose that the role of RSC in making CDSs nucleosomes accessible (Figure 3) is important for efficient transcription. In *rsc8* cells, polymerases might struggle to negotiate nucleosomes in CDSs leading to altered Pol II profiles at the 3' ends. This idea is supported by the observations that RSC is enriched in transcribed CDSs, and that Pol II shows significant interaction with more accessible nucleosomes genome-wide.

DISCUSSION

Our data show that RSC recruitment to coding sequences makes nucleosomes accessible in a manner that may promote transcription. In support of this, we show that the genes which showed RSC occupancies in their CDSs were also the ones most affected by impairing RSC function. Furthermore, RSC-bound nucleosomes within CDSs were highly susceptible to MNase digestion, suggesting that remodeling by RSC could make DNA accessible to transcribing Pol II. Consistent with this idea, we find that the Pol II-bound nucleosomes were digested to a greater extent than the canonical nucleosomes in the same regions.

A recent *in vitro* study showed that RSC preferentially remodels nucleosomes derived from promoters and NDRs (Cakiroglu et al., 2019). In agreement with this, we found that -2, -1, and +1 nucleosomes displayed a greater proportion of shorter MPDFs compared to all other nucleosomes genome-wide (Figure 1E). This suggests that promoter nucleosomes are amongst the most accessible in the genome. Indeed, the MNase ChIP-seq data revealed that RSC localizes to promoter nucleosomes. Additionally, RSC_Nucs in these promoters were more sensitive to MNase digestion than nucleosomes not bound to RSC (Figure 3C). This implies that promoter nucleosomes are direct targets for RSC remodeling activity, which could aid in evicting or clearing promoter nucleosomes to promote transcription (Klein-Brill et al., 2019; Kubik et al., 2019; Rawal et al., 2018). Taken together, these data suggests that promoter nucleosomes are direct targets for RSC remodeling activity.

Intriguingly, RSC localization to -1_Nucs nucleosomes and NDRs did not correlate with Pol II occupancies, nor with the Pol II occupancy defects caused by Rsc8 depletion (Figures 2G and 4C).

This is surprising, because cells with compromised RSC function display substantially increased nucleosomes in NDRs, and NDRs are considered to be important for transcription initiation (Klein-Brill et al., 2019; Kubik et al., 2019; Rawal et al., 2018). Indeed, we observed shallower NDRs upon depleting RSC even at the bottom 10% of transcribed genes compared to the WT cells. These data suggest that RSC plays a general, global role in promoting NDR formation by scanning for displaced nucleosomes, in order to eject or push the nucleosomes to precise positions. As such, it is expected that RSC would interact transiently with nucleosomes flanking the NDRs of all genes, regardless of the transcriptional status of each gene. Consistent with this, loss of RSC function resulted in NDR filling genome-wide in a manner independent of transcription status (Figures 4C-4E). Immunoprecipitation-independent methods such as "CUT&RUN" (Skene and Henikoff, 2017) and ChEC-seq (Zentner et al., 2015) have shown that RSC localizes to -1 and +1 nucleosomes for the majority of genes, and that RSC loss leads to the movement of -1 and +1 nucleosomes towards NDRs genome-wide (Brahma and Henikoff, 2019; Klein-Brill et al., 2019; Kubik et al., 2019; Kubik et al., 2018; Ocampo et al., 2019; Parnell et al., 2015). These methods detected RSC signal at more genes than conventional ChIP, providing evidence that RSC may indeed interact transiently with promoter nucleosomes at these genes. Collectively, these data indicate that RSC plays a general role at promoters that is independent of transcription.

However, at the smaller subset of Pro-target genes, low Pol II occupancies were observed, indicating that RSC may play a role in promoting transcription of lowly expressed genes. Consistent with this, Pol II occupancies at Pro-targets were reduced upon Rsc8 depletion (Figure 4D). In contrast to other promoter nucleosomes, RSC occupancy at +1_Nucs strongly correlated

with Pol II occupancies and with the transcriptional defects resulting from depleting Rsc8 (Figure 2G). These correlations suggest that RSC may stably interact with the +1 nucleosome of transcribing genes. This makes sense, since +1 nucleosomes must be repositioned or evicted for PIC assembly (Klein-Brill et al., 2019). Overall, while RSC occupancy at some promoters does seem to correlate with transcription, RSC may have a more global role at promoters that is largely transcription-independent.

Given that a single nucleosome is a potent barrier for Pol II elongation, mechanisms must exist to make nucleosomes in CDSs accessible to elongating polymerases. The presence of shorter (<120 bp) MPDFs in CDSs of transcribed genes indicates generation of MNase-sensitive/accessible nucleosomes (Figure 1F). However, it is not clear which remodelers might help in this process. RSC and SWI/SNF have both histone sliding and histone eviction activities (Boeger et al., 2004; Clapier et al., 2017; Montel et al., 2011) and are shown to be present in CDSs of transcribed genes (Ganguli et al., 2014; Rawal et al., 2018; Spain et al., 2014; Vinayachandran et al., 2018; Yen et al., 2012). In addition, RSC is shown to promote Pol II elongation, *in vitro*, through acetylated nucleosomes (Carey et al., 2006). It has been reported that RSC bound nucleosomes in NDRs are "fragile," suggesting that RSC might expose DNA and makes nucleosomes sensitive to MNase digestion (Brahma and Henikoff, 2019; Kubik et al., 2015). While there is controversy regarding fragile nucleosomes in NDRs (Chereji et al., 2017), it is clear that RSC make nucleosomes accessible (Cakiroglu et al., 2019; Clapier et al., 2017). Considering that promoter nucleosomes are the most accessible, we propose that RSC generates accessible "promoter-like" nucleosome in CDSs. In support of this, we show that RSC-bound nucleosomes displayed very heterogenous MPDF lengths, which might represent remodeling intermediates. As one might expect, we find a

higher proportion of shorter MPDFs at very highly transcribed genes, including at the RPGs. The profile for nucleosomes (MNase inputs) did not show the fragment heterogeneity that is observed for the RSC_Nucs, implying that only a small fraction of nucleosomes within a gene are accessible at any given time. We think that the nucleosomes immediately downstream of the elongating polymerases might be targeted by RSC and rendered accessible, whereas, other nucleosomes will be in a canonical conformation (largely inaccessible; MPDF >130 bp). In agreement with this, the Pol II_Nucs also displayed significant proportion of shorter MPDFs similar to that observed for the RSC_Nucs, suggesting that Pol II does access MNase-sensitive nucleosomes in CDSs.

Previous studies, including ours, have provided support for the idea that RSC interacts with elongating Pol II via the Rsc4 subunit or in a manner dependent on Pol II CTD phosphorylation (Soutourina et al., 2006; Spain et al., 2014). Rsc4 has also been shown to recognize acetylated H3K14 *in vitro*. It is therefore possible that RSC uses Rsc4, along with other bromodomain-containing subunits, to recognize Pol II-proximal nucleosomes, which are transiently acetylated by the SAGA and NuA4 HAT complexes (Ginsburg et al., 2009; Govind et al., 2007; Kasten et al., 2004). Acetylation of nucleosomes has also been implicated in enhancing remodeling by the RSC complex (Chatterjee et al., 2015; Chatterjee et al., 2011). Thus, RSC-bound nucleosomes might resemble promoter nucleosomes in that these nucleosomes will be hyperacetylated and susceptible to MNase digestion. The remodeling by RSC may be limited to nucleosome immediately downstream of the elongating Pol II, since nucleosomes upstream of the Pol II will be deacetylated by Hos2-Set1 and Rpd3(S)-Set2 pathway (Carrozza et al., 2005; Govind et al., 2010; Kim and Buratowski, 2009). These complexes are shown to interact with phosphorylated Pol II and deacetylates CDSs nucleosomes in a manner dependent on histone methylation. The

idea that RSC provides transient access to nucleosomal DNA in an acetylation-dependent manner might also provide an explanation as to why cryptic-transcription initiation occurs from within CDSs in cells deficient of HDAC or histone methyltransferase function (Carrozza et al., 2005). Altogether, our data suggests that RSC-mediating remodeling of nucleosomes in CDSs promotes transcription.

ACKNOWLEDGEMENT

We thank Dr. Alan Hinnebusch, Dr. David Clark and Dr. Gabriel Zentner for providing useful comments on the manuscript. CKG was supported by NIH grants R01 GM095514 and R15GM126449.

AUTHOR CONTRIBUTIONS

Conceptualization, CKG and EB; Methodology, CKG, JK, and EB; Investigation; CKG, JK, EB, KD, CR; Writing, CKG, EB and KD; Supervision, CKG; Administration, CKG, Funding Acquisition, CKG.

DECLARATION OF INTEREST

The authors declare no competing interests.

REFERENCES

Badis, G., Chan, E.T., van Bakel, H., Pena-Castillo, L., Tillo, D., Tsui, K., Carlson, C.D., Gossett, A.J., Hasinoff, M.J., Warren, C.L.*, et al.* (2008). A library of yeast transcription factor motifs reveals a widespread function for Rsc3 in targeting nucleosome exclusion at promoters. Mol Cell *32*, 878-887.

Boeger, H., Griesenbeck, J., Strattan, J.S., and Kornberg, R.D. (2004). Removal of promoter nucleosomes by disassembly rather than sliding in vivo. Mol Cell *14*, 667-673.

Brahma, S., and Henikoff, S. (2019). RSC-Associated Subnucleosomes Define MNase-Sensitive Promoters in Yeast. Mol Cell *73*, 238-249.e233.

Cairns, B.R., Lorch, Y., Li, Y., Zhang, M., Lacomis, L., Erdjument-Bromage, H., Tempst, P., Du, J., Laurent, B., and Kornberg, R.D. (1996). RSC, an essential, abundant chromatin-remodeling complex. Cell *87*, 1249-1260.

Cakiroglu, A., Clapier, C.R., Ehrensberger, A.H., Darbo, E., Cairns, B.R., Luscombe, N.M., and Svejstrup, J.Q. (2019). Genome-wide reconstitution of chromatin transactions reveals that RSC preferentially disrupts H2AZ-containing nucleosomes. Genome Res *29*, 988-998.

Carey, M., Li, B., and Workman, J.L. (2006). RSC exploits histone acetylation to abrogate the nucleosomal block to RNA polymerase II elongation. Mol Cell *24*, 481-487.

Carrozza, M.J., Li, B., Florens, L., Suganuma, T., Swanson, S.K., Lee, K.K., Shia, W.J., Anderson, S., Yates, J., Washburn, M.P.*, et al.* (2005). Histone H3 methylation by Set2 directs deacetylation of coding regions by Rpd3S to suppress spurious intragenic transcription. Cell *123*, 581-592.

Chatterjee, N., North, J.A., Dechassa, M.L., Manohar, M., Prasad, R., Luger, K., Ottesen, J.J., Poirier, M.G., and Bartholomew, B. (2015). Histone Acetylation near the Nucleosome Dyad Axis Enhances Nucleosome Disassembly by RSC and SWI/SNF. Mol Cell Biol *35*, 4083-4092.

Chatterjee, N., Sinha, D., Lemma-Dechassa, M., Tan, S., Shogren-Knaak, M.A., and Bartholomew, B. (2011). Histone H3 tail acetylation modulates ATP-dependent remodeling through multiple mechanisms. Nucleic Acids Res *39*, 8378-8391.

Chereji, R.V., Ocampo, J., and Clark, D.J. (2017). MNase-Sensitive Complexes in Yeast: Nucleosomes and Non-histone Barriers. Mol Cell *65*, 565-577 e563.

Chereji, R.V., Ramachandran, S., Bryson, T.D., and Henikoff, S. (2018). Precise genome-wide mapping of single nucleosomes and linkers in vivo. Genome Biol *19*, 19.

Churchman, L.S., and Weissman, J.S. (2011). Nascent transcript sequencing visualizes transcription at nucleotide resolution. Nature *469*, 368-373.

Clapier, C.R., and Cairns, B.R. (2009). The biology of chromatin remodeling complexes. Annu Rev Biochem *78*, 273-304.

Clapier, C.R., Iwasa, J., Cairns, B.R., and Peterson, C.L. (2017). Mechanisms of action and regulation of ATP-dependent chromatin-remodelling complexes. Nat Rev Mol Cell Biol *18*, 407-422.

Clapier, C.R., Kasten, M.M., Parnell, T.J., Viswanathan, R., Szerlong, H., Sirinakis, G., Zhang, Y., and Cairns, B.R. (2016). Regulation of DNA Translocation Efficiency within the Chromatin Remodeler RSC/Sth1 Potentiates Nucleosome Sliding and Ejection. Mol Cell *62*, 453-461.

Dion, M.F., Kaplan, T., Kim, M., Buratowski, S., Friedman, N., and Rando, O.J. (2007). Dynamics of Replication-Independent Histone Turnover in Budding Yeast. Science *315*, 1405-1408.

Farnung, L., Vos, S.M., and Cramer, P. (2018). Structure of transcribing RNA polymerase II-nucleosome complex. Nat Commun *9*, 5432.

Ganguli, D., Chereji, R.V., Iben, J.R., Cole, H.A., and Clark, D.J. (2014). RSC-dependent constructive and destructive interference between opposing arrays of phased nucleosomes in yeast. Genome Res *24*, 1637-1649.
Ginsburg, D.S., Govind, C.K., and Hinnebusch, A.G. (2009). NuA4 lysine acetyltransferase Esa1 is targeted to coding regions and stimulates transcription elongation with Gcn5. Mol Cell Biol *29*, 6473-6487.
Govind, C.K., Qiu, H., Ginsburg, D.S., Ruan, C., Hofmeyer, K., Hu, C., Swaminathan, V., Workman, J.L., Li, B., and Hinnebusch, A.G. (2010). Phosphorylated Pol II CTD recruits multiple HDACs, including Rpd3C(S), for methylation-dependent deacetylation of ORF nucleosomes. Mol Cell *39*, 234-246.
Govind, C.K., Zhang, F., Qiu, H., Hofmeyer, K., and Hinnebusch, A.G. (2007). Gcn5 promotes acetylation, eviction, and methylation of nucleosomes in transcribed coding regions. Mol Cell *25*, 31-42.
Hartley, P.D., and Madhani, H.D. (2009a). Mechanisms that Specify Promoter Nucleosome Location and Identity. Cell *137*, 445-458.
Hartley, P.D., and Madhani, H.D. (2009b). Mechanisms that specify promoter nucleosome location and identity. Cell *137*, 445-458.
Henikoff, J.G., Belsky, J.A., Krassovsky, K., MacAlpine, D.M., and Henikoff, S. (2011). Epigenome characterization at single base-pair resolution. Proceedings of the National Academy of Sciences *108*, 18318.
Kasten, M., Szerlong, H., Erdjument-Bromage, H., Tempst, P., Werner, M., and Cairns, B.R. (2004). Tandem bromodomains in the chromatin remodeler RSC recognize acetylated histone H3 Lys14. EMBO J *23*, 1348-1359.
Kim, T., and Buratowski, S. (2009). Dimethylation of H3K4 by Set1 Recruits the Set3 Histone Deacetylase Complex to 5' Transcribed Regions. Cell *137*, 259-272.
Kireeva, M.L., Walter, W., Tchernajenko, V., Bondarenko, V., Kashlev, M., and Studitsky, V.M. (2002). Nucleosome remodeling induced by RNA polymerase II: loss of the H2A/H2B dimer during transcription. Mol Cell *9*, 541-552.
Klein-Brill, A., Joseph-Strauss, D., Appleboim, A., and Friedman, N. (2019). Dynamics of Chromatin and Transcription during Transient Depletion of the RSC Chromatin Remodeling Complex. Cell Rep *26*, 279-292.e275.
Koerber, R.T., Rhee, H.S., Jiang, C., and Pugh, B.F. (2009). Interaction of transcriptional regulators with specific nucleosomes across the Saccharomyces genome. Mol Cell *35*, 889-902.
Krietenstein, N., Wal, M., Watanabe, S., Park, B., Peterson, C.L., Pugh, B.F., and Korber, P. (2016). Genomic Nucleosome Organization Reconstituted with Pure Proteins. Cell *167*, 709-721 e712.
Kubik, S., Bruzzone, M.J., Challal, D., Dreos, R., Mattarocci, S., Bucher, P., Libri, D., and Shore, D. (2019). Opposing chromatin remodelers control transcription initiation frequency and start site selection. Nat Struct Mol Biol *26*, 744-754.
Kubik, S., Bruzzone, M.J., Jacquet, P., Falcone, J.L., Rougemont, J., and Shore, D. (2015). Nucleosome Stability Distinguishes Two Different Promoter Types at All Protein-Coding Genes in Yeast. Mol Cell *60*, 422-434.
Kubik, S., Bruzzone, M.J., and Shore, D. (2017). Establishing nucleosome architecture and stability at promoters: Roles of pioneer transcription factors and the RSC chromatin remodeler. Bioessays *39*.

Kubik, S., O'Duibhir, E., de Jonge, W.J., Mattarocci, S., Albert, B., Falcone, J.L., Bruzzone, M.J., Holstege, F.C.P., and Shore, D. (2018). Sequence-Directed Action of RSC Remodeler and General Regulatory Factors Modulates +1 Nucleosome Position to Facilitate Transcription. Mol Cell *71*, 89-102 e105.
Kujirai, T., Ehara, H., Fujino, Y., Shirouzu, M., Sekine, S.-i., and Kurumizaka, H. (2018). Structural basis of the nucleosome transition during RNA polymerase II passage. Science *362*, 595.
Kulaeva, O.I., Gaykalova, D.A., and Studitsky, V.M. (2007). Transcription through chromatin by RNA polymerase II: histone displacement and exchange. Mutation research *618*, 116-129.
Lorch, Y., LaPointe, J.W., and Kornberg, R.D. (1987). Nucleosomes inhibit the initiation of transcription but allow chain elongation with the displacement of histones. Cell *49*, 203-210.
Montel, F., Castelnovo, M., Menoni, H., Angelov, D., Dimitrov, S., and Faivre-Moskalenko, C. (2011). RSC remodeling of oligo-nucleosomes: an atomic force microscopy study. Nucleic acids research *39*, 2571-2579.
Musladin, S., Krietenstein, N., Korber, P., and Barbaric, S. (2014). The RSC chromatin remodeling complex has a crucial role in the complete remodeler set for yeast PHO5 promoter opening. Nucleic Acids Res *42*, 4270-4282.
Ocampo, J., Chereji, R.V., Eriksson, P.R., and Clark, D.J. (2019). Contrasting roles of the RSC and ISW1/CHD1 chromatin remodelers in RNA polymerase II elongation and termination. Genome Res *29*, 407-417.
Parnell, T.J., Schlichter, A., Wilson, B.G., and Cairns, B.R. (2015). The chromatin remodelers RSC and ISW1 display functional and chromatin-based promoter antagonism. Elife *4*, e06073.
Ramachandran, S., Ahmad, K., and Henikoff, S. (2017). Transcription and Remodeling Produce Asymmetrically Unwrapped Nucleosomal Intermediates. Mol Cell *68*, 1038-1053 e1034.
Ramachandran, S., and Henikoff, S. (2016a). Nucleosome dynamics during chromatin remodeling in vivo. Nucleus *7*, 20-26.
Ramachandran, S., and Henikoff, S. (2016b). Transcriptional Regulators Compete with Nucleosomes Post-replication. Cell *165*, 580-592.
Ramachandran, S., Zentner, G.E., and Henikoff, S. (2015). Asymmetric nucleosomes flank promoters in the budding yeast genome. Genome Res *25*, 381-390.
Rawal, Y., Chereji, R.V., Qiu, H., Ananthakrishnan, S., Govind, C.K., Clark, D.J., and Hinnebusch, A.G. (2018). SWI/SNF and RSC cooperate to reposition and evict promoter nucleosomes at highly expressed genes in yeast. Genes Dev *32*, 695-710.
Shukla, M.S., Syed, S.H., Montel, F., Faivre-Moskalenko, C., Bednar, J., Travers, A., Angelov, D., and Dimitrov, S. (2010). Remosomes: RSC generated non-mobilized particles with approximately 180 bp DNA loosely associated with the histone octamer. Proceedings of the National Academy of Sciences *107*, 1936.
Skene, P.J., and Henikoff, S. (2017). An efficient targeted nuclease strategy for high-resolution mapping of DNA binding sites. Elife *6*.
Soutourina, J., Bordas-Le Floch, V., Gendrel, G., Flores, A., Ducrot, C., Dumay-Odelot, H., Soularue, P., Navarro, F., Cairns, B.R., Lefebvre, O*., et al.* (2006). Rsc4 connects the chromatin remodeler RSC to RNA polymerases. Mol Cell Biol *26*, 4920-4933.
Spain, M.M., Ansari, S.A., Pathak, R., Palumbo, M.J., Morse, R.H., and Govind, C.K. (2014). The RSC complex localizes to coding sequences to regulate Pol II and histone occupancy. Mol Cell *56*, 653-666.

Spain, M.M., and Govind, C.K. (2011). A role for phosphorylated Pol II CTD in modulating transcription coupled histone dynamics. Transcription *2*, 78-81.
Suter, B., Schnappauf, G., and Thoma, F. (2000). Poly(dA.dT) sequences exist as rigid DNA structures in nucleosome-free yeast promoters in vivo. Nucleic Acids Res *28*, 4083-4089.
Vinayachandran, V., Reja, R., Rossi, M.J., Park, B., Rieber, L., Mittal, C., Mahony, S., and Pugh, B.F. (2018). Widespread and precise reprogramming of yeast protein-genome interactions in response to heat shock. Genome Res.
Weber, C.M., Ramachandran, S., and Henikoff, S. (2014). Nucleosomes are context-specific, H2A.Z-modulated barriers to RNA polymerase. Mol Cell *53*, 819-830.
Yen, K., Vinayachandran, V., Batta, K., Koerber, R.T., and Pugh, B.F. (2012). Genome-wide nucleosome specificity and directionality of chromatin remodelers. Cell *149*, 1461-1473.
Zentner, G.E., Kasinathan, S., Xin, B., Rohs, R., and Henikoff, S. (2015). ChEC-seq kinetics discriminates transcription factor binding sites by DNA sequence and shape in vivo. Nat Commun *6*, 8733.

LEGENDS TO THE FIGURES

Figure 1. Nucleosomes in transcribed coding Sequences are more susceptible to MNase digestion.

A) Fragment length distribution of MNase-digested DNA sequences from two biological replicates.

B) Heatmaps depicting average nucleosome occupancies of the two replicates +/- 1000 bp relative to the transcription start sites (TSS). The genes were sorted on the basis of average Pol II (Rpb3) ChIP-seq occupancies in their CDSs.

C) Heatmap depicting Pol II occupancies, which were determined by ChIP-seq for Rpb3 using sonicated chromatin (n=5746).

D) Schematics showing potential generation of MNase protected DNA fragments (MPDFs) from nucleosomes. MNase digestion of a wrapped nucleosome would likely generate MPDFs ~130-160 bp, whereas a remodeled nucleosomes might be more accessible, leading to shorter MPDFs (<130 bp).

E) MPDF profiles for fragment lengths ranging from 130-160 bp, <120 bp-110, <110-100 bp, <100-90 bp, and <90 bp for 5746 genes.

F) Metagene profile showing the average occupancies of MPDFs for the top (Pol II-T10) and bottom 10% (Pol II-B10) Pol II-occupied genes. MPDFs sizes <130 bp and >130 bp are plotted +/- 1000 bp around the TSS.

Figure 2. RSC enrichment in CDSs but not in promoters correlate with transcription.

A) A genome-browser screen-shot showing normalized ChIP-seq reads nucleosomes (black), RSC (red), and RPb3 (green) obtained from MNase-digested chromatin, as well as for Rpb3 (blue) obtained from sonicated chromatin. Biological replicates are shown.

B) Heatmap depicting RSC MNase ChIP-seq occupancies normalized to nucleosome occupancies obtained from MNase-seq data for 5746 genes sorted by decreasing Pol II occupancy.

C) Heatmaps showing RSC occupancies (top panel) and nucleosome occupancies (bottom panel) for the bottom- and top- 10% Pol II-occupied genes, as well as for the top 10% of genes where RSC was located at the promoter (Promoter-targets, occupancy encompassing -1 nucleosome and NDR). All heatmaps were sorted based on decreasing Poll II occupancies and is constituted of 576 genes.

D) Metagene profiles depicting nucleosome-normalized RSC (top) and nucleosome occupancies (bottom) for the indicated gene-sets.

E) Scatterplot showing the correlation between nucleosome-normalized RSC occupancies in promoters and in CDSs, and average Pol II occupancies for all genes (n=5746).

F) Heatmaps depicting the average Pol II ChIP-seq occupancy over gene bodies for the indicated gene-sets.

G) Scatter plot showing correlation between RSC occupancies in -1 and +1 nucleosomes with average Pol II occupancies genome-wide.

Figure 3. RSC associates with both full-length and shorter MPDFs.

A and B): Metagene profile showing normalized reads of MPDFs corresponding to the nucleosomes (MNase inputs; Nuc) and RSC-bound nucleosomes (RSC MNase ChIP-seq; RSC) for the bottom 10% (A) and top 10% Pol II-occupied genes (B).

C and D): Heatmaps depicting 2D-occupancies of MPDF distribution around the TSS, with MPDFs shown on the Y-axis. MPDFs from nucleosomes (C) and RSC-bound nucleosomes (D) at the bottom 10% Pol II-occupied genes, Pro-target genes, and top 10% Pol II-occupied genes. (E) Metagene profiles depicting the relative amount of fragment lengths for the nucleosomes (left panel) and RSC-bound nucleosome MPDFs observed in (C) and (D) (right panel). The profiles for ribosomal protein genes (RPGs) are also included.

Figure 4. Loss of RSC impairs transcription of genes displaying high RSC in their CDSs.

A) Heatmap showing Pol II occupancies from Pol-II MNase ChIP-seq data, sorted by decreasing Pol II occupancies.

B) Scatterplot depicting correlation between Rpb3 ChIP-seq occupancies from MNase and sonicated chromatin.

C) 2-D occupancy plots showing MPDF distribution obtained from Rpb3-bound nucleosomes for the top 10% of Pol II-occupied genes.

D) Scatterplot showing the correlation between Rpb3 and RSC occupancies in promoters and CDSs with the changes in input-normalized Rpb3 occupancy upon depleting Rsc8 subunit (*rsc8*) of the RSC complex (data from (Ocampo et al., 2019)).

E) Boxplot comparing the changes in Pol II occupancies between WT and *rsc8* for the top 10% RSC affected genes, Promoter-target genes, the top 10% RSC-occupied genes, the top 10% Pol II-occupied genes, and all genes. Numbers above each boxplot indicate the median Pol II occupancies of genes within each category.

F and G): Metagene profiles showing MNase-seq reads for nucleosomes for wildtype and *rsc8* (data from (Ocampo et al., 2019)) at the bottom 10% Pol II-occupied genes and at Promoter-target genes (F), as well as at the top 10% Pol II-occupied genes (G).

LEGENDS TO THE SUPPLEMENTAL FIGURES

Figure S1: MNase-seq and Pol II ChIP-seq in WT cell.

A) Heatmaps depicting nucleosome occupancy in +/- 1000 bp relative to the transcription start sites (TSS) for the two biological replicates. The genes were sorted based on the average Pol II (Rpb3) occupancies in the coding sequences.

B) Plot showing the dyad occupancies for the two MNase-seq replicates.

C) Heatmap depicting Pol II occupancies around the TSS (+/- 1kb) which were determined by ChIP-seq for the Pol II (Rpb3) using sonicated chromatin occupancies (n=5746). The genes were sorted on the basis of the average Rpb3 occupancies in their CDSs.

Figure S2. RSC enrichment in CDSs but not in promoters correlate with transcription.

A) Metagene profile showing occupancies of nucleosomes (MNase inputs), and RSC and Rpb3 occupancies normalized to nucleosome occupancies for the ribosomal protein genes.

B) 5746 genes were sorted by decreasing Pol II occupancy and grouped in deciles. Average occupancy of RSC in CDs for each decile is shown.

C) Venn diagram showing overlap between the top 10% genes which show highest Rpb3 (Pol II-T10) and RSC occupancies (RSC-T10) in their coding sequences.

D) Box plot showing Rpb3 occupancies for the indicated gene-sets. The bottom 10% Pol II occupied genes showing lowest and ribosomal protein genes (RPGs) shows the highest.

F) Boxplot showing very similar dAdT content for the Pol II-B10, Pro-target and Pol II-T10. The average dAdT content is shown for +/- 250 bp relative to the transcription start sites.

Figure S3. RSC associates with both full-length and shorter MPDFs.

A and B): Heatmaps depicting 2D occupancies of MPDF distribution around the TSS, with MPDFs shown on the Y-axis. Heatmaps for the MPDFs from nucleosomes (MNase-seq) (A) and RSC-bound nucleosomes (B) at the bottom 10% Pol II-occupied genes, Pro-target genes, top 10% Pol II-occupied genes, and ribosomal protein genes (RPGs) are shown.

(C-E) Metagene profiles depicting the relative coverage of MPDFs lengths of the RSC-bound nucleosome vs total nucleosomes for the Pol II-B10 (C), Pro-targets (D) and Pol II-T10 (E) are shown.

Figure S4. Loss of RSC impairs transcription of genes displaying high RSC in their CDSs.

A) Venn diagram showing that RSC-affected genes shows significant overlap with transcribed genes (Pol II-T10) but not with the Pro-targets.

B) Heatmaps showing average Pol II occupancies in the CDSs of the Pol II-T10, RSC-T10, Pro-targets, and Pol II-B10 (left panels) and the differences in Pol II occupancies on depleting Rsc8 at these gene-sets compared to the WT cells (right panels).

C) Rpb3 ChIP-seq profiles for the WT and Rsc8-depleted cells (*rsc8*) for the top 10% Pol II-occupied and top 10% genes showing maximum RSC occupancy in -1_Nuc and NDRs (Pro).

D) Changes in Pol II occupancies at the Pol II-T10 and Pro-targets upon depletion of Rsc8

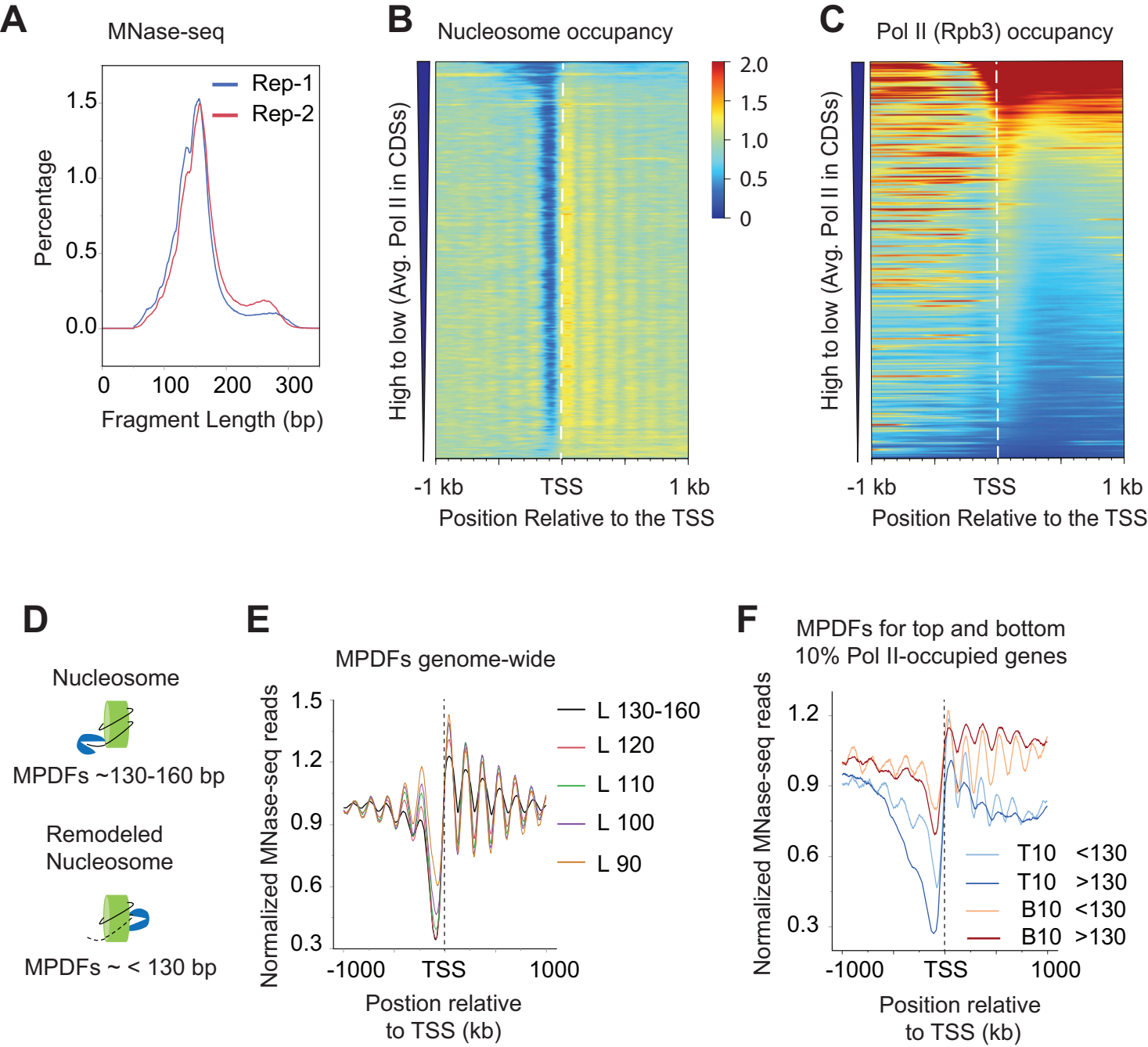
A
MNase-seq
Rep-1
Rep-2
Percentage
1.5
1.0
0.5
0.0
0
100
200
300
Fragment Length (bp)
B
Nucleosome occupancy
High to low (Avg. Pol II in CDSs)
2.0
1.5
1.0
0.5
0
-1 kb
TSS
1 kb
Position Relative to the TSS
C
Pol II (Rpb3) occupancy
High to low (Avg. Pol II in CDSs)
-1 kb
TSS
1 kb
Position Relative to the TSS
D
Nucleosome
MPDFs ~130-160 bp
Remodeled Nucleosome
MPDFs ~ < 130 bp
E
MPDFs genome-wide
Normalized MNase-seq reads
1.5
1.2
0.9
0.6
0.3
-1000
TSS
1000
Postion relative to TSS (kb)
L 130-160
L 120
L 110
L 100
L 90
F
MPDFs for top and bottom 10% Pol II-occupied genes
Normalized MNase-seq reads
1.2
0.9
0.6
0.3
-1000
TSS
1000
Position relative to TSS (kb)
T10 <130
T10 >130
B10 <130
B10 >130

Figure 1

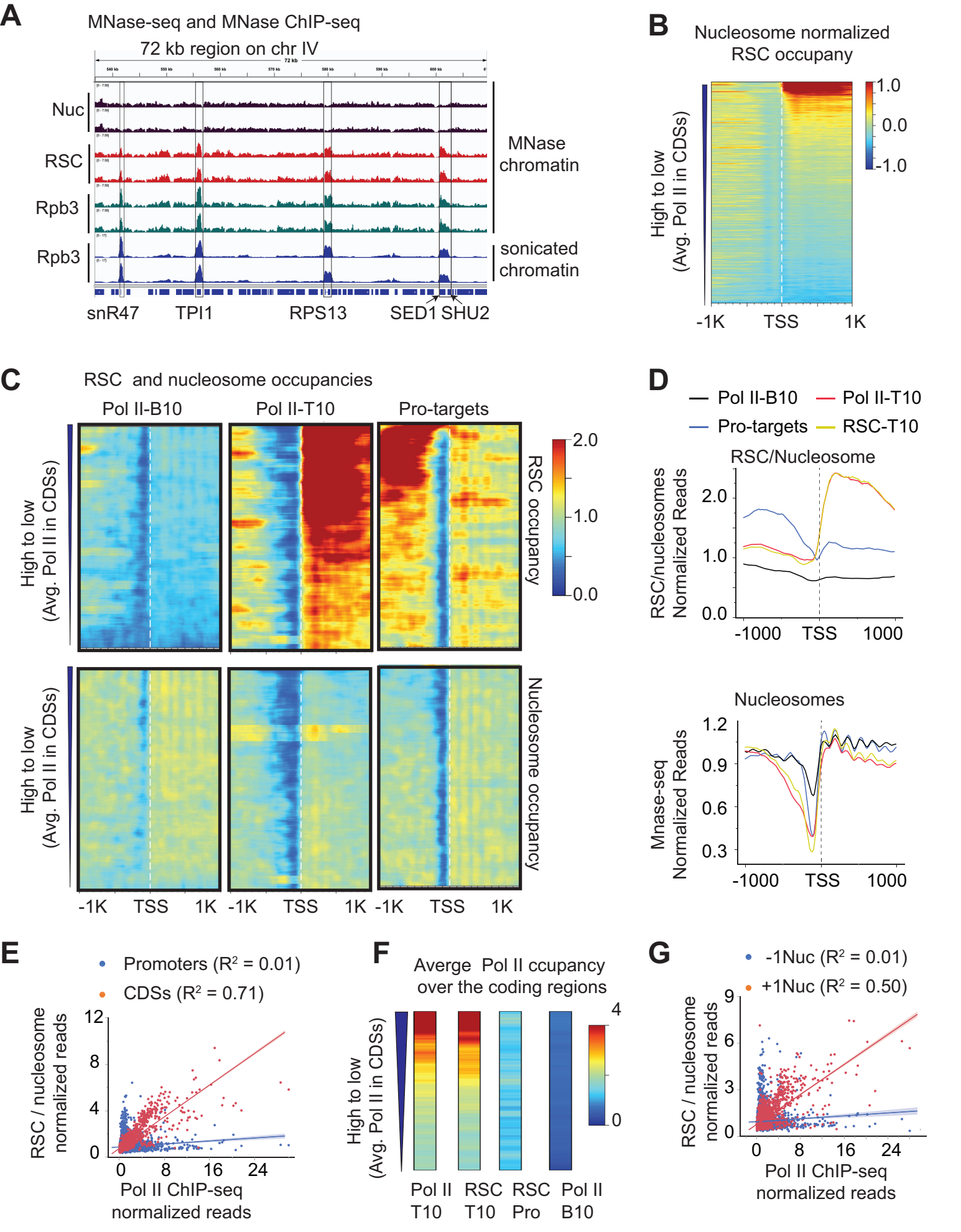
A
MNase-seq and MNase ChIP-seq
72 kb region on chr IV
Nuc
RSC
Rpb3
Rpb3
MNase chromatin
sonicated chromatin
snR47
TPI1
RPS13
SED1
SHU2
B
Nucleosome normalized RSC occupany
High to low (Avg. Pol II in CDSs)
1.0
0.0
-1.0
-1K
TSS
1K
C
RSC and nucleosome occupancies
Pol II-B10
Pol II-T10
Pro-targets
RSC occupancy
Nucleosome occupancy
2.0
1.0
0.0
D
Pol II-B10
Pol II-T10
Pro-targets
RSC-T10
RSC/Nucleosome
RSC/nucleosomes Normalized Reads
Nucleosomes
Mnase-seq Normalized Reads
-1000
TSS
1000
E
Promoters (R² = 0.01)
CDSs (R² = 0.71)
RSC / nucleosome normalized reads
Pol II ChIP-seq normalized reads
F
Averge Pol II ccupancy over the coding regions
Pol II T10
RSC T10
RSC Pro
Pol II B10
G
-1Nuc (R² = 0.01)
+1Nuc (R² = 0.50)
RSC / nucleosome normalized reads
Pol II ChIP-seq normalized reads

Figure 2

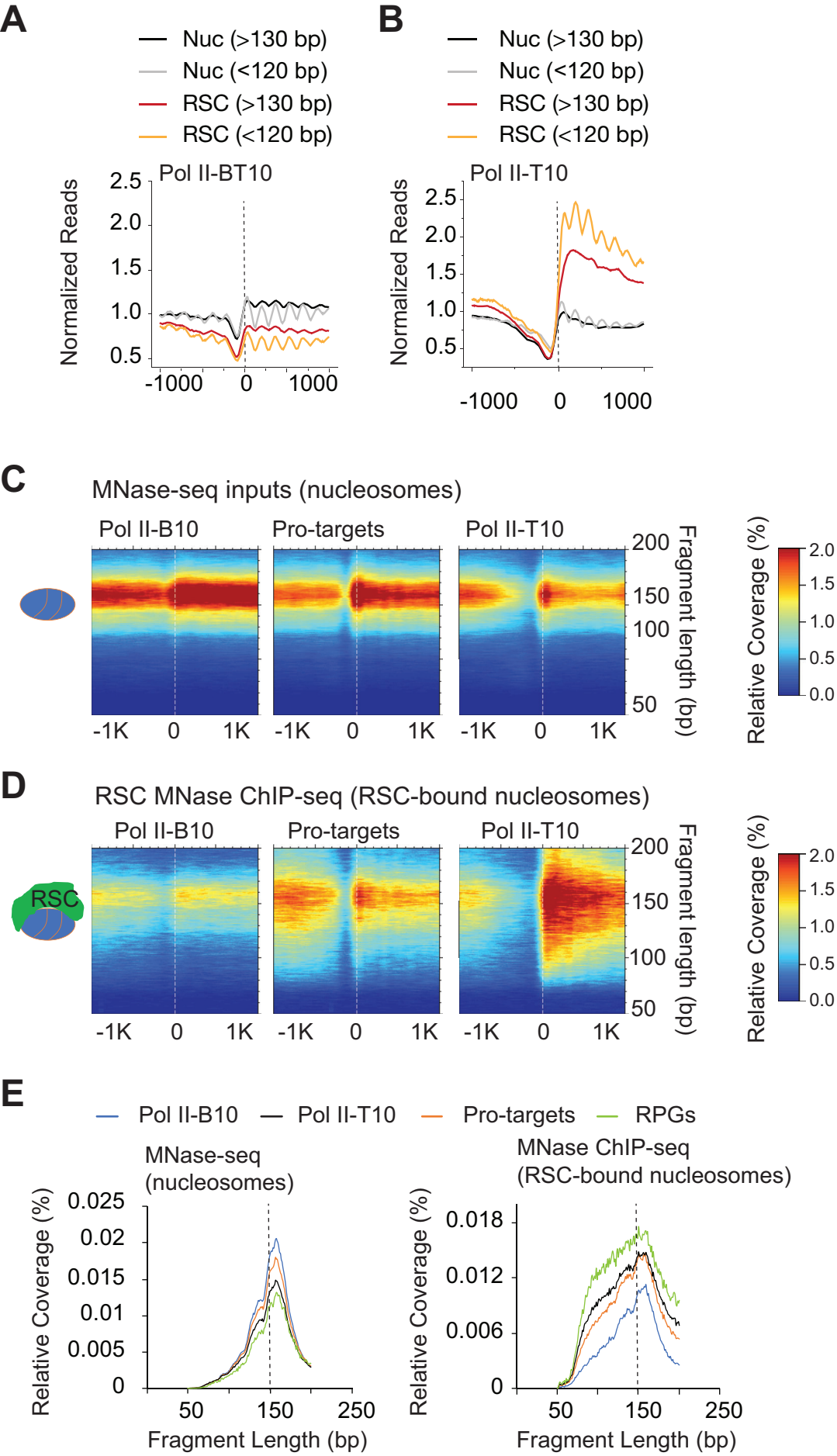
A
Nuc (>130 bp)
Nuc (<120 bp)
RSC (>130 bp)
RSC (<120 bp)
Pol II-BT10
Normalized Reads
2.5
2.0
1.5
1.0
0.5
-1000
0
1000
B
Nuc (>130 bp)
Nuc (<120 bp)
RSC (>130 bp)
RSC (<120 bp)
Pol II-T10
Normalized Reads
2.5
2.0
1.5
1.0
0.5
-1000
0
1000
C
MNase-seq inputs (nucleosomes)
Pol II-B10
Pro-targets
Pol II-T10
-1K
0
1K
200
150
100
50
Fragment length (bp)
Relative Coverage (%)
2.0
1.5
1.0
0.5
0.0
D
RSC MNase ChIP-seq (RSC-bound nucleosomes)
RSC
Pol II-B10
Pro-targets
Pol II-T10
-1K
0
1K
200
150
100
50
Fragment length (bp)
Relative Coverage (%)
2.0
1.5
1.0
0.5
0.0
E
Pol II-B10
Pol II-T10
Pro-targets
RPGs
MNase-seq
(nucleosomes)
Relative Coverage (%)
0.025
0.02
0.015
0.01
0.005
0
50
150
250
Fragment Length (bp)
MNase ChIP-seq
(RSC-bound nucleosomes)
Relative Coverage (%)
0.018
0.012
0.006
0
50
150
250
Fragment Length (bp)

Figure 3

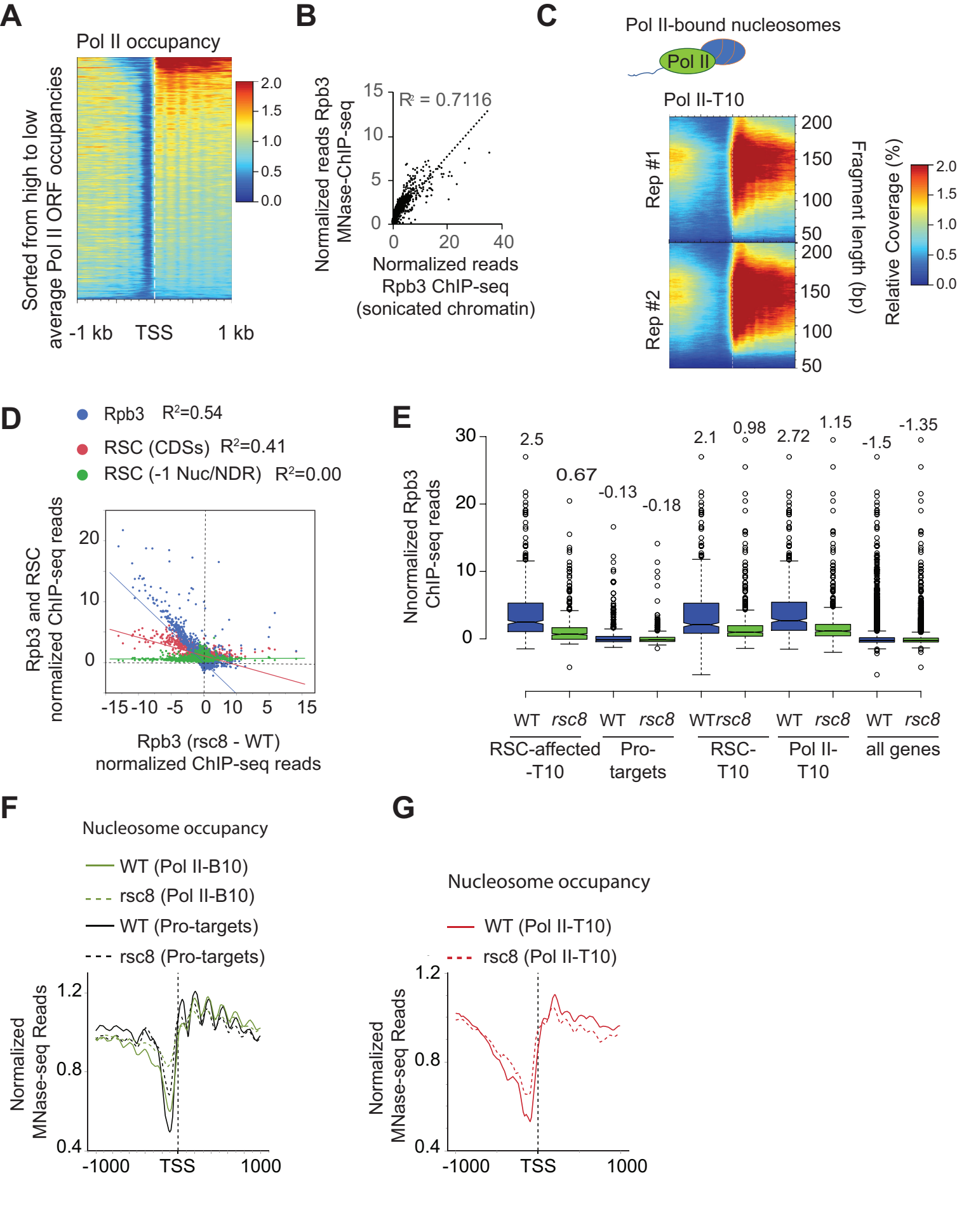
A
Pol II occupancy
Sorted from high to low average Pol II ORF occupancies
-1 kb
TSS
1 kb
2.0
1.5
1.0
0.5
0.0
B
R² = 0.7116
Normalized reads Rpb3 MNase-ChIP-seq
Normalized reads Rpb3 ChIP-seq (sonicated chromatin)
C
Pol II-bound nucleosomes
Pol II
Pol II-T10
Rep #1
Rep #2
Fragment length (bp)
Relative Coverage (%)
D
Rpb3 R²=0.54
RSC (CDSs) R²=0.41
RSC (-1 Nuc/NDR) R²=0.00
Rpb3 and RSC normalized ChIP-seq reads
Rpb3 (rsc8 - WT) normalized ChIP-seq reads
E
Nnormalized Rpb3 ChIP-seq reads
2.5
0.67
-0.13
-0.18
2.1
0.98
2.72
1.15
-1.5
-1.35
WT rsc8 WT rsc8 WT rsc8 WT rsc8 WT rsc8
RSC-affected -T10
Pro-targets
RSC-T10
Pol II-T10
all genes
F
Nucleosome occupancy
WT (Pol II-B10)
rsc8 (Pol II-B10)
WT (Pro-targets)
rsc8 (Pro-targets)
Normalized MNase-seq Reads
G
Nucleosome occupancy
WT (Pol II-T10)
rsc8 (Pol II-T10)
Normalized MNase-seq Reads

Figure 4

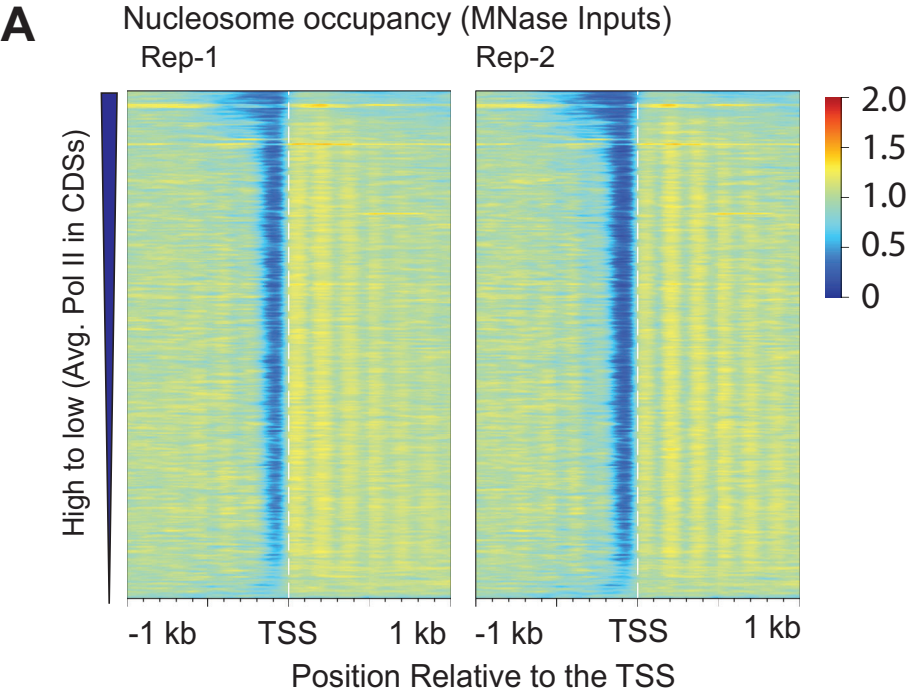
A
Nucleosome occupancy (MNase Inputs)
Rep-1
Rep-2
High to low (Avg. Pol II in CDSs)
2.0
1.5
1.0
0.5
0
-1 kb
TSS
1 kb
-1 kb
TSS
1 kb
Position Relative to the TSS

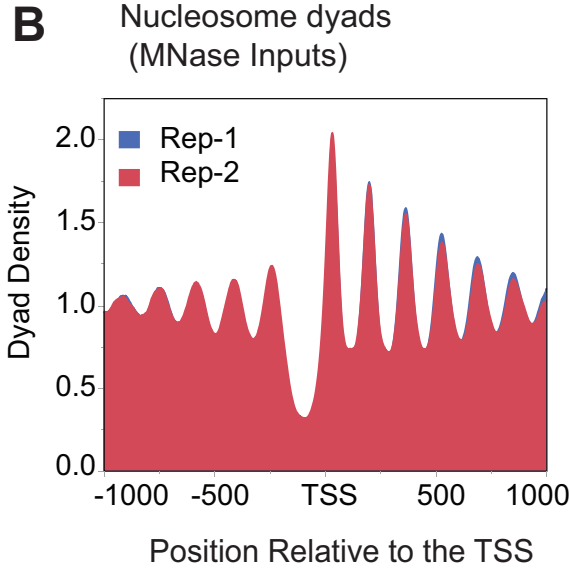
B
Nucleosome dyads
(MNase Inputs)
Rep-1
Rep-2
Dyad Density
2.0
1.5
1.0
0.5
0.0
-1000
-500
TSS
500
1000
Position Relative to the TSS

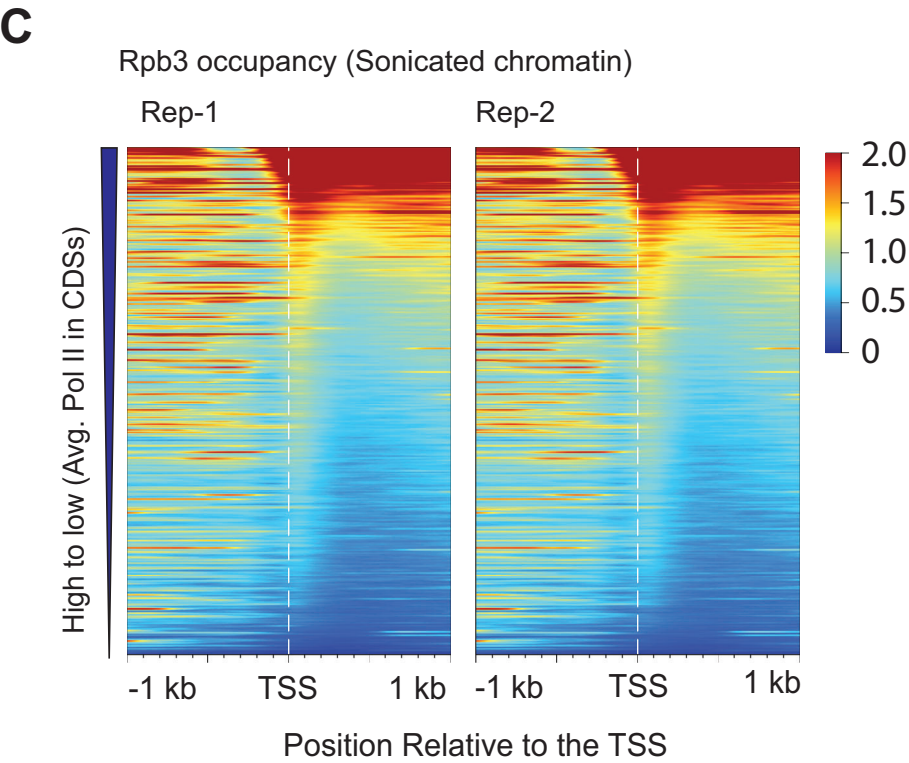
C
Rpb3 occupancy (Sonicated chromatin)
Rep-1
Rep-2
High to low (Avg. Pol II in CDSs)
2.0
1.5
1.0
0.5
0
-1 kb
TSS
1 kb
-1 kb
TSS
1 kb
Position Relative to the TSS

Figure S1

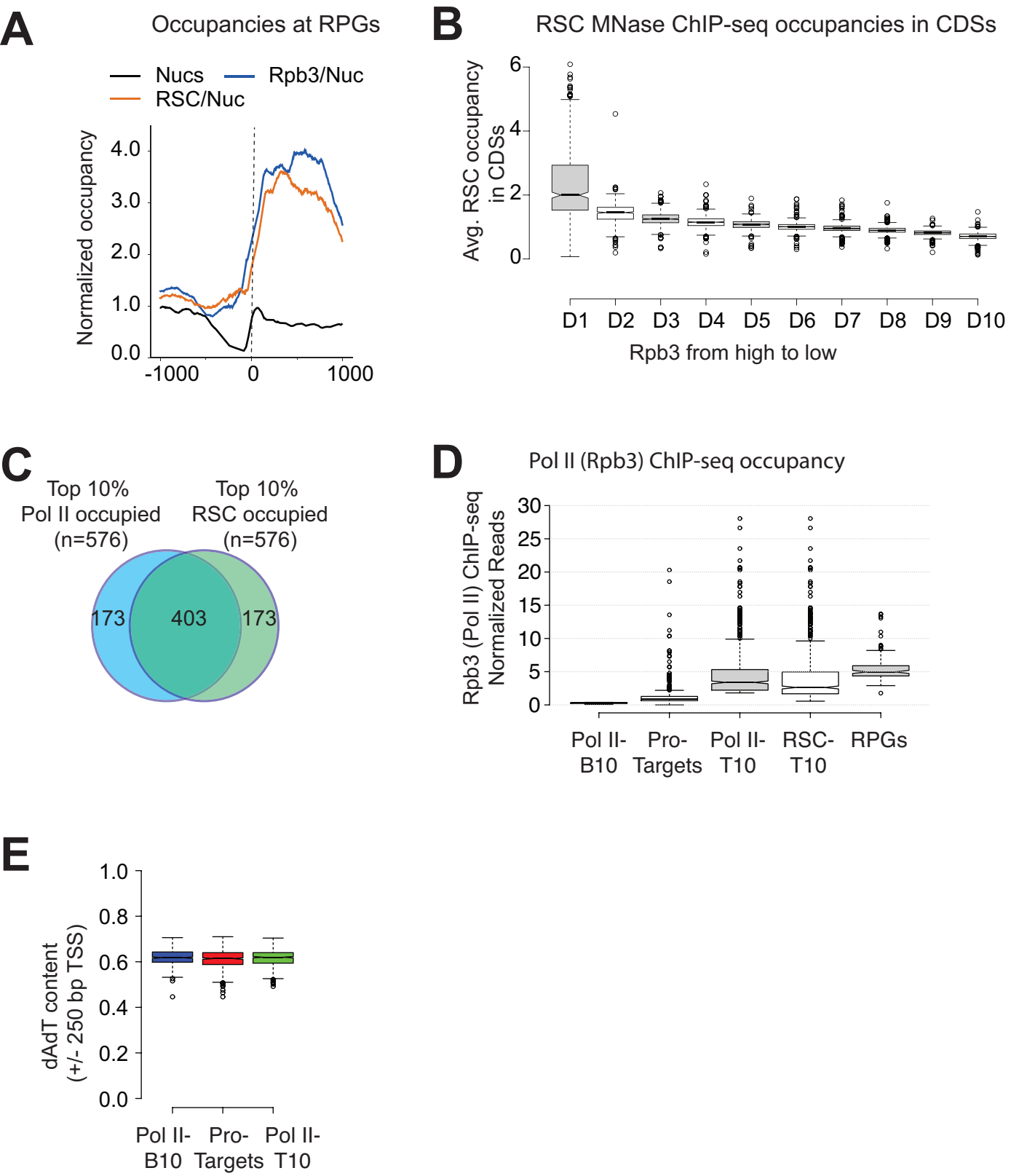
A
Occupancies at RPGs
Nucs
Rpb3/Nuc
RSC/Nuc
Normalized occupancy
4.0
3.0
2.0
1.0
0.0
-1000
0
1000
B
RSC MNase ChIP-seq occupancies in CDSs
Avg. RSC occupancy in CDSs
6
4
2
0
D1
D2
D3
D4
D5
D6
D7
D8
D9
D10
Rpb3 from high to low
C
Top 10% Pol II occupied (n=576)
Top 10% RSC occupied (n=576)
173
403
173
D
Pol II (Rpb3) ChIP-seq occupancy
Rpb3 (Pol II) ChIP-seq Normalized Reads
30
25
20
15
10
5
0
Pol II-B10
Pro-Targets
Pol II-T10
RSC-T10
RPGs
E
dAdT content (+/- 250 bp TSS)
1.0
0.8
0.6
0.4
0.2
0.0
Pol II-B10
Pro-Targets
Pol II-T10

Figure S2

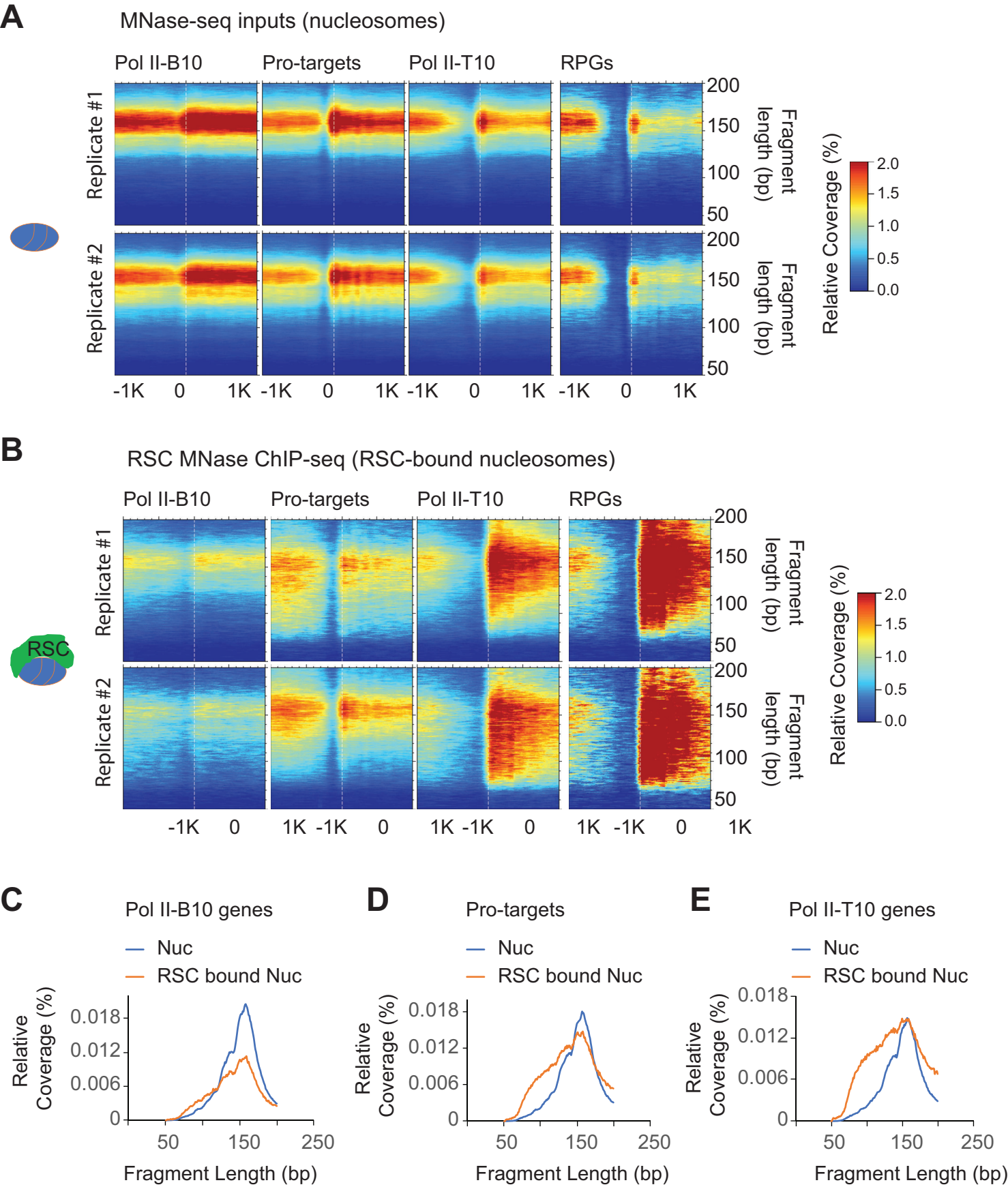
A
MNase-seq inputs (nucleosomes)
Pol II-B10
Pro-targets
Pol II-T10
RPGs
Replicate #1
Replicate #2
Fragment length (bp)
200
150
100
50
-1K
0
1K
Relative Coverage (%)
2.0
1.5
1.0
0.5
0.0
B
RSC MNase ChIP-seq (RSC-bound nucleosomes)
RSC
C
Pol II-B10 genes
Nuc
RSC bound Nuc
Relative Coverage (%)
0.018
0.012
0.006
0
Fragment Length (bp)
D
Pro-targets
E
Pol II-T10 genes

Figure S3

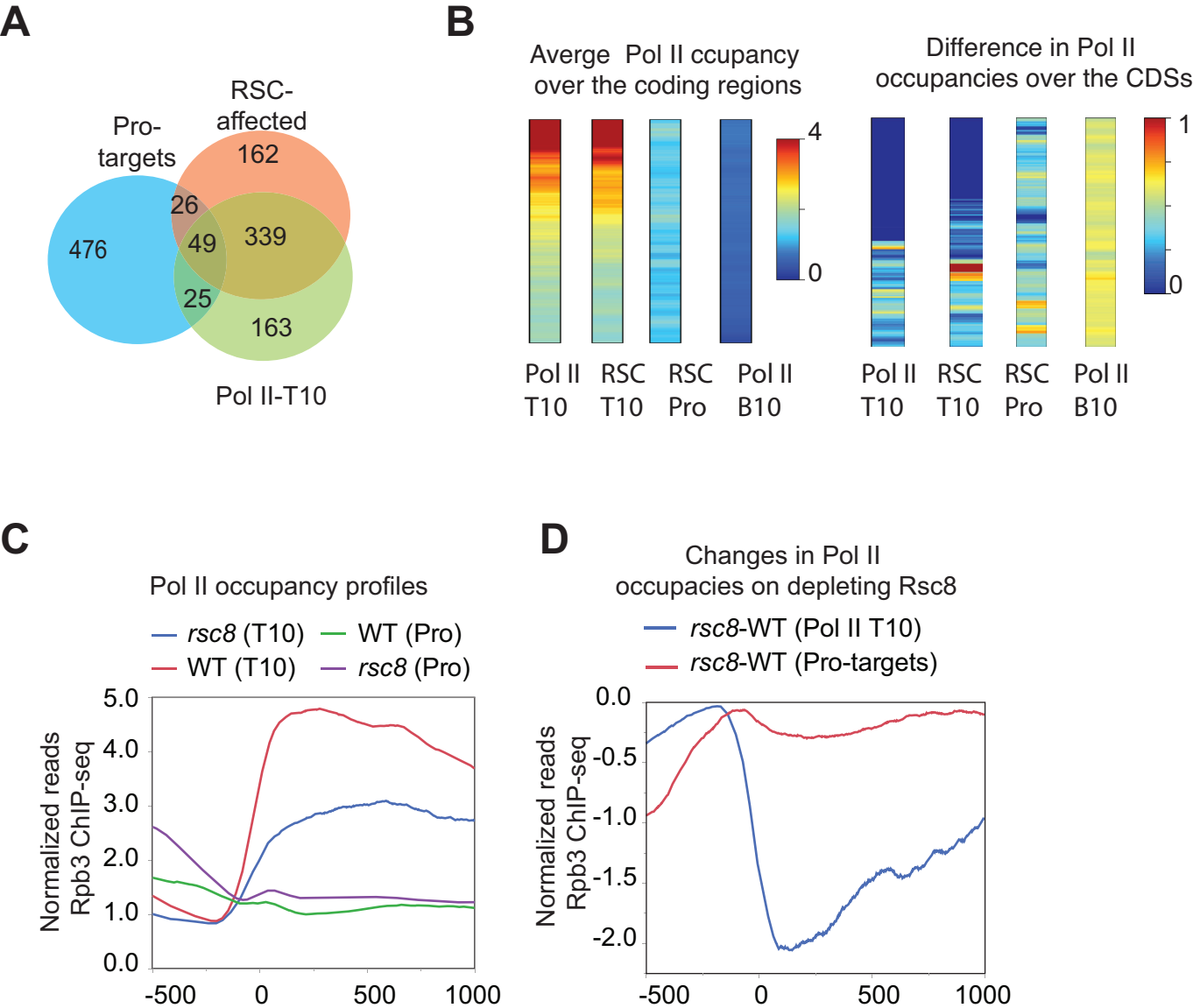
A
Pro-targets
RSC-affected
162
26
476
49
339
25
163
Pol II-T10
B
Averge Pol II ccupancy over the coding regions
Difference in Pol II occupancies over the CDSs
4
0
1
0
Pol II T10
RSC T10
RSC Pro
Pol II B10
Pol II T10
RSC T10
RSC Pro
Pol II B10
C
Pol II occupancy profiles
rsc8 (T10)
WT (Pro)
WT (T10)
rsc8 (Pro)
Normalized reads Rpb3 ChIP-seq
5.0
4.0
3.0
2.0
1.0
0.0
-500
0
500
1000
D
Changes in Pol II occupacies on depleting Rsc8
rsc8-WT (Pol II T10)
rsc8-WT (Pro-targets)
Normalized reads Rpb3 ChIP-seq
0.0
-0.5
-1.0
-1.5
-2.0
-500
0
500
1000

Figure S4

Experimental Model and Subject Details

All *Saccharomyces cerevisiae* strains used in this study are derived from the BY4741. The cells were grown in YPD at 30°C.

Yeast Strain Construction and Growth Conditions

The *S. cerevisiae* strains used in this study are listed in Supplementary Table S1. Myc-tagged strains were generated as described (Govind et al., 2012). Briefly, the plasmid pFA6a-13xMyc-His3MX6 was used as a template to PCR amplify the 13xMyc using primers containing homologous sequences flanking the stop codon of the *STH1*. The amplified DNA was used to transformation, and the colonies were selected on SC plates lacking histidine (SC/His$^-$). The transformants were confirmed by PCR and expression of tagged protein by Western blot.

Cells that were successfully tagged were then grown in YPD to an absorbance A_{600} of 0.7-0.8 before being crosslinked as described previously (Govind et al., 2012). Briefly, 11 ml of the crosslinking solution (50 mM HEPES-KOH [pH 7.5], 1 mM EDTA, 100 mM NaCl, 11% formaldehyde) was added to 100 ml culture. Cultures were for 15 minutes at room temperature with intermittent shaking, and the crosslinking was quenched by adding 15 ml of 2.5M glycine. Cells were collected by centrifugation at 4000 rpm at 4°C for 5 mins, and were washed twice with chilled 1X TBS. Cell pellets were stored at -80°C until further use.

MNase Digestion:

Crosslinked cell pellets were thawed on ice and resuspended in pre-chilled 500 µl FA-lysis buffer (50 mM HEPES-KOH [pH 7.5], 1 mM EDTA, 140 mM NaCl, 1% Triton X-100, 0.1% sodium deoxycholate) containing protease inhibitors. Approximately 500 µl of acid-washed glass beads was added to the resuspended cells, and cells were disrupted for 45 min in a cold room. The cell-extracts were collected by centrifugation, and beads were washed once with 500 µl FA-lysis buffer, and the supernatant was pooled with the cell-extracts. The cell-extracts were centrifuged for 30 min at 4°C, and the pellet was washed twice with FA-lysis buffer, and subsequently resuspended in 600 µl of NPS buffer with 1mM β-marcaptoethanol (0.5 mM spermidine, 0.075% IGEPAL, 50 mM NaCl, 10 mM Tris-HCl; pH 7.5, 5 mM $MgCl_2$, 1 mM $CaCl_2$). MNase digestion was carried out at 30°C for 12 minutes with different MNase concentrations. The digestion was stopped by adding EDTA to final concentration of 10 mM, and transferring tubes to ice for 10 min. To determine the extent of digestion, DNA was purified from 50 µl aliquots of MNase-digested chromatin. The chromatin samples showing ~80% mono-nucleosomes (DNA fragments corresponding to 150 bp) were used for ChIP and library preparation.

Chromatin Immunoprecipitation

ChIP was performed using a slightly modified protocol described previously {Govind, 2012 #1717}. 60 μl of anti-mouse magnetic beads was washed PBS/BSA (5 mg/ml BSA), and incubated with 3 μl of anti-Myc or Anti-Rpb3 antibodies in 150 µl of PBS/BSA for 3 hours. Post-incubation, the beads were washed twice with PBS/BSA and were incubated with 300 μl of MNase-digested chromatin for 3.5 hours. 150 μl MNase chromatin was set aside as MNase-inputs. The beads were subsequently washed with the following buffers: once with PBS/BSA, twice each with FA-lysis buffer, twice with wash-buffer II (50mM HEPES-KOH, 500 mM NaCl, 1 mM EDTA, 0.1% sodium deoxycholate, 1% Triton-X 100), wash-buffer III (10mM Tris-Hcl (pH8.0), 250 mM LiCl, 1mM EDTA, 0.5% sodium deoxycholate, 0.5% NP-40 substitute), and finally once with 1X TE. The immunoprecipitated complexes were eluted at 65°C once by elution buffer I (50mM Tris-HCl, 10mM EDTA, 1% SDS) for 10 minutes and then by Elution Buffer II (10mM Tris-HCl, 1mM EDTA, 0.67% SDS) for 15 minutes at 65°C. The eluents were pooled and incubated overnight in a 65°C water bath for reverse crosslinking along with the MNase-inputs. The following day, the samples were treated with 5 μl of proteinase K (20mg/ml, Ambion, cat# AM2548) for 2 hours and DNA from the immunoprecipitates was extracted twice with chloroform:isoamyl alcohol (IAA), and ethanol precipitated overnight at -80°C. The DNA was resuspended in 50 µl 1X TE/RNAse (10 µg/ml).

Library Preparation and sequencing

ChIP DNA (7-10 ng) as well as the corresponding MNase-input DNA (50 ng) were processed for generating libraries for MNase-seq and ChIP-seq using the NEBNext Ultra II Library prep kit for Illumina. BIOO Scientific NEXTFLEX ChIP-Seq barcode oligos were ligated and the library was amplified according to the manufacturer instructions. The DNA library was gel purified and sequenced in Illumina HiSeq-4K in paired-end mode (50bp) at the University of Michigan Advanced Genomics Core Facility in Ann Arbor, MI, USA.

Data Analysis

Sequence were trimmed to remove adapters using the Cutadapt (parameter: -m 20), aligned to the S. cerevisiae genome (SacCer3) Bowtie2 (parameters -X 1000 –very-sensitive –no-mix –no-unal). Samtools was used to sort, index, and remove PCR duplicates from the .bam files. The MNase-seq and MNase ChIP-seq bam files were analyzed using BamR (https://github.com/rchereji/bamR). The 2D-occupancy heatmaps were generated using the plot2DO.R. The fragments were aligned to their 5' end. Metagene profiles and scatterplots were in JMP. Boxplots were generated using the website http://shiny.chemgrid.org/boxplotr/. Venn diagrams were made using http://www.biovenn.nl/.

Data and Software Availability

The accession numbers for the raw and analyzed data reported in this paper are GEOXXXX.

Table S1: Strains used in this Study

Name	Parent	Genotype	Reference
CGY 2	BY4741	*MATa his3Δ1 leu2Δ0 met15Δ0 ura3Δ0 STH1-myc13::HIS3*	This study
F729	BY4741	*MATa his3Δ1 leu2Δ0 met15Δ0 ura3Δ0*	Research Genetics
YPE468	W303	*MATaade2-1can1-100his3-11,15leu2-3,112trp1-1ura3-1RAD5+rsc8::KanMX-GALp-HA3-RSC8*	(Ocampo et al., 2019)